Cell

Kid-Mediated Chromosome Compaction Ensures Proper Nuclear Envelope Formation

Miho Ohsugi,[1] Kenjiro Adachi,[2,4] Reiko Horai,[2,5] Shigeru Kakuta,[2] Katsuko Sudo,[2,6] Hayato Kotaki,[2] Noriko Tokai-Nishizumi,[1] Hiroshi Sagara,[3] Yoichiro Iwakura,[2] and Tadashi Yamamoto[1,*]
[1]Division of Oncology, Department of Cancer Biology
[2]Division of Cell Biology, Center for Experimental Medicine
[3]Laboratory of Proteomics, Institute of Medical Science
The University of Tokyo, Minato-ku, Tokyo, 108-8639, Japan
[4]Present address: Laboratory for Pluripotent Cell Studies, RIKEN Center for Developmental Biology, Kobe, Hyogo, 650-0047, Japan.
[5]Present address: National Eye Institute, NIH, Bethesda, MD, 20892, USA.
[6]Present address: Animal Research Center, Tokyo Medical University, Shinjuku-ku, Tokyo, 160-8402, Japan.
*Correspondence: tyamamot@ims.u-tokyo.ac.jp
DOI 10.1016/j.cell.2008.01.029

SUMMARY

Toward the end of mitosis, neighboring chromosomes gather closely to form a compact cluster. This is important for reassembling the nuclear envelope around the entire chromosome mass but not individual chromosomes. By analyzing mice and cultured cells lacking the expression of chromokinesin Kid/kinesin-10, we show that Kid localizes to the boundaries of anaphase and telophase chromosomes and contributes to the shortening of the anaphase chromosome mass along the spindle axis. Loss of Kid-mediated anaphase chromosome compaction often causes the formation of multinucleated cells, specifically at oocyte meiosis II and the first couple of mitoses leading to embryonic death. In contrast, neither male meiosis nor somatic mitosis after the morula-stage is affected by Kid deficiency. These data suggest that Kid-mediated anaphase/telophase chromosome compaction prevents formation of multinucleated cells. This protection is especially important during the very early stages of development, when the embryonic cells are rich in ooplasm.

INTRODUCTION

To transmit genetic information faithfully, replicated chromosomes must be properly condensed, aligned, and segregated to daughter cells during mitosis. In higher eukaryotic cells that undergo open mitosis, the structural elements of the nuclear envelope (NE), including the nuclear lamina, nuclear pore complexes (NPCs), and nuclear membranes are disassembled at the end of prophase and reassembled around the segregated chromosomes at late anaphase and telophase (Burke and Ellenberg, 2002). NE reassembly is a complex multistep process that starts with the direct association and accumulation of membrane vesicles or ER-like membrane cisternae, and certain components of NPCs at the chromosomal surface, followed by membrane fusion, NPC reassembly, and nuclear lamina formation (Burke and Ellenberg, 2002; Hetzer et al., 2005). All anaphase chromosomes are segregated by poleward movement in a synchronized manner, or else lagging chromosomes will assemble their own NEs, resulting in micronuclei. Therefore, it is important to clarify the exact mechanism by which all the chromosomes are incorporated into a single daughter nucleus at the end of mitosis. A recent study demonstrated that the chromatin-occupied volume decreased to the lowest level at late anaphase in mammalian cells, which appears to be important for the formation of a single daughter nucleus with a smooth surface (Mora-Bermudez et al., 2007). However, the underlying mechanism and the physiological consequences of such anaphase/telophase chromosome compaction on cell division in vivo remain obscure.

In vertebrates, unfertilized eggs are arrested at metaphase of the second meiosis (meta II) and fertilization triggers completion of the second meiotic division and emission of the second polar body. Then NEs are assembled separately around maternal and paternal chromosomes, forming separate haploid male and female pronuclei that eventually fuse to produce diploid zygotes during the first mitosis. The zygote undergoes several rounds of specialized mitosis called cleavage division under the influence of ooplasm, namely depending exclusively on maternal proteins and mRNAs (Ciemerych and Sicinski, 2005; O'Farrell et al., 2004). In contrast to the *Xenopus* cleavage cycles that rapidly oscillate between S and M phase 12 times without checkpoint controls and zygotic gene expression (Clute and Masui, 1997; Newport and Dasso, 1989; Newport and Kirschner, 1982), the mouse cleavage cycle includes G1 and G2 phases (Ciemerych and Sicinski, 2005) and the spindle assemble checkpoint is activated even in 1-cell embryos (Siracusa et al., 1980). In addition, major zygotic gene expression takes place as early as the 2-cell stage in mice (Flach et al., 1982). Thus, it appears that the early cleavage cycle of mammalian embryos and the somatic cell cycle progress according to the same scheme. Indeed, there is little difference between the two (Ciemerych and Sicinski, 2005).

The chromokinesin Kid/kinesin-10, a plus-end directed microtubule-based motor with both microtubule- and DNA-binding

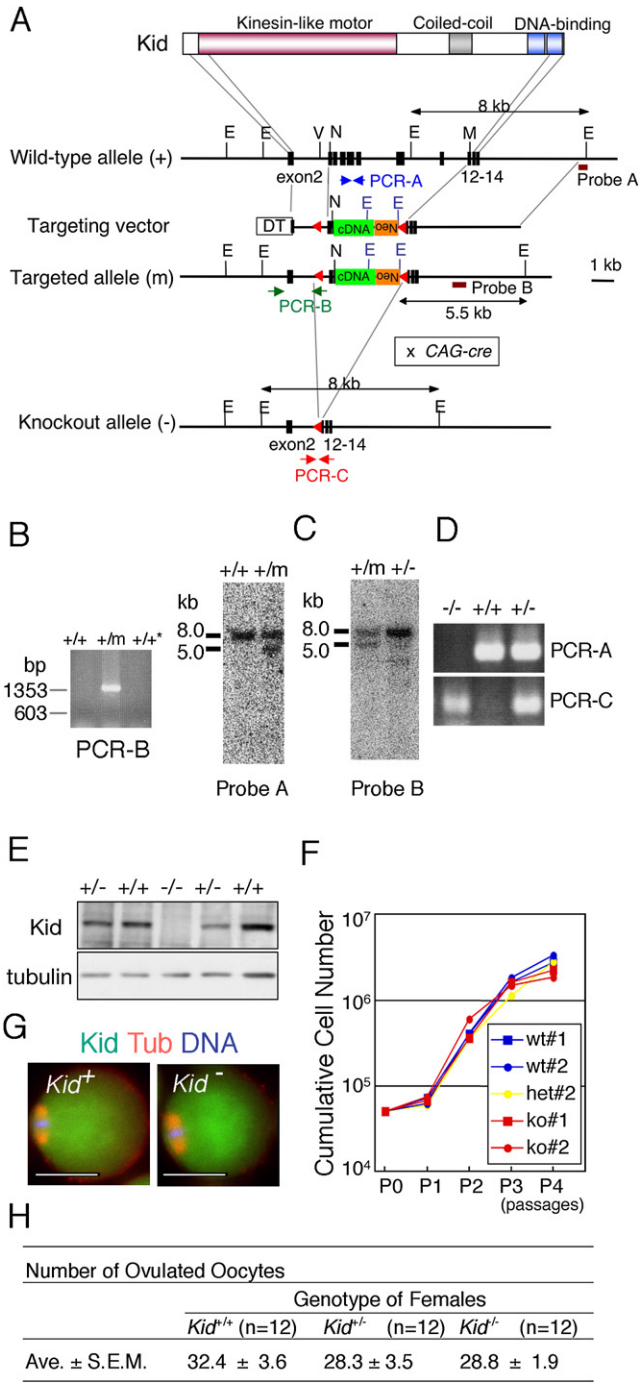

Number of Ovulated Oocytes			
	Genotype of Females		
	$Kid^{+/+}$ (n=12)	$Kid^{+/-}$ (n=12)	$Kid^{-/-}$ (n=12)
Ave. ± S.E.M.	32.4 ± 3.6	28.3 ± 3.5	28.8 ± 1.9

Figure 1. Kid Is Critical for Early Embryonic Development but Is Dispensable for Later Embryonic Growth and Meiosis in Mice

(A) Schematic representations of the structures of Kid protein, wild-type allele, targeting vector, and homologous recombinant (targeted) and Cre-loxP recombinant (knockout) alleles with relevant restriction sites. The probes for Southern blotting and positions of PCR primers are indicated. Red triangles indicate the positions of *loxP* sites. cDNA, *Kid* cDNA covering from *Nco* I site (N) within exon 4 to stop codon; Neo, neomycin-resistance gene; E, *Eco R*I site; M, *Msc* I site; V, *Eco R*V site.

(B) PCR and Southern blot analysis of targeted ES clones. Genomic DNAs from wild-type (+/+), homologous recombinant (+/m), or random integrated (+/+*) ES cell clones were used as template for PCR using primer set B (left panel), or were digested with *Eco R*I and hybridized with Probe A (right panel).

(C) Southern blot analysis of genomic DNA prepared from $Kid^{+/m}$ or $Kid^{+/-}$ mice with Probe B.

(D) Genotyping PCR analysis of $Kid^{+/+}$, $Kid^{+/-}$ or $Kid^{-/-}$ mice using primer sets A and C.

(E) Whole-cell lysates of MEFs derived from $Kid^{+/+}$, $Kid^{+/-}$ or $Kid^{-/-}$ E14.5 embryo were subjected to immunoblotting with the indicated antibodies.

(F) Proliferation of $Kid^{+/+}$(wt), $Kid^{+/-}$ (het) or $Kid^{-/-}$ (ko) MEFs using a 3T3 protocol. wt#1 and ko#1, and wt#2, het#2, and ko#2 were derived from littermates, respectively.

(G) Immunostaining of meta II-arrested oocyte collected from the oviduct of $Kid^{+/+}$ or $Kid^{-/-}$ female mice for Kid, β-tubulin and DNA. The scale bars represent 40 μm.

(H) Comparison of the numbers of ovulated oocytes per mouse after superovulation treatment.

domains, is one of the mitotic motors (Tokai et al., 1996). Kid is conserved among vertebrates and has been implicated in chromosome movement along microtubules during prometaphase and metaphase (Antonio et al., 2000; Funabiki and Murray, 2000; Levesque and Compton, 2001; Tokai-Nishizumi et al., 2005). Upon the onset of anaphase, Xkid in *Xenopus* egg extracts is almost completely degraded (Antonio et al., 2000; Funabiki and Murray, 2000). In contrast, a significant amount of Kid exists on anaphase chromosomes in mammalian cells (Ohsugi et al., 2003; Tokai et al., 1996). Although depletion of Kid causes pre-anaphase delay, it does not affect the kinetochore-microtubule attachment and the majority of cells eventually enter anaphase (Tokai-Nishizumi et al., 2005; Zhu et al., 2005). During anaphase and telophase, Kid-depletion causes lagging chromosomes and the formation of malformed nuclei at somewhat high frequency, suggesting a role of Kid in anaphase chromosome dynamics, although the details have not been clarified (Tokai-Nishizumi et al., 2005; Zhu et al., 2005).

In this study, we addressed the role of Kid by analyzing mice and HeLa cells lacking its expression. Kid deficiency causes loss of the tight gathering of anaphase chromosomes, which often leads to the formation of micro- or multinucleated cells, specifically in very early-stage embryos, leading to death, while neither mitotic proliferation during post-morula development nor gamete formation is affected. We further show that Kid localizes together with microtubules in the interstices between adjacent anaphase chromosomes and helps to hold individual chromosomes together during segregation to form a compact chromosome mass at telophase. We propose that mammalian early-stage embryos, which are under significant influence of the ooplasm with high NE-assembly activity, specifically require Kid-mediated compaction of the anaphase chromosome mass to prevent the formation of multinucleated cells.

RESULTS

Kid Is Critical for Early Embryonic Development but Is Dispensable for Later Embryonic Growth and Meiosis in Mice

To elucidate the effects of Kid deficiency on cell division during mammalian development, we generated Kid-deficient mice by gene targeting. We first generated conditional knockout mice in which exons 3–12 of *Kid* were replaced by a loxP-flanked DNA segment containing intact exon 3, partial exon 4 fused in frame to *Kid* cDNA and a neomycin-resistance cassette (Figure 1A).

Table 1. Genotype Analysis

Genotype and Genetic Background of Parents		Number (Percent of Total) with Genotype			
Female × Male	Stage	+/+	+/−	−/−	Total
+/− × +/− < 129/B6 mix >	3 weeks	91 (25.6%)	223 (62.8%)	41 (11.6%)	355
	E14.5	19 (25.7%)	45 (60.8%)	10 (13.5%)	74
	E9.5	28 (26.7%)	63 (60.0%)	14 (13.3%)	105
+/− × −/− < 129/B6 mix >	3 weeks	–	132 (64.1%)	74 (35.9%)	206
	Blastocyst	–	40 (69.0%)	18 (31.0%)	58
	2–8 cells	–	48 (44.4%)	60 (55.6%)	108
−/− × +/− < 129/B6 mix >	3 weeks	–	94 (75.2%)	31 (24.8%)	125
	2–8 cells	–	8 (36.4%)	14 (63.6%)	22
+/− × +/− < B6 (N8) >	3 weeks	52 (31.1%)	101 (60.5%)	14 (8.4%)	167
+/− × −/− < B6 (N8) >	3 weeks	–	77 (80.2%)	19 (19.8%)	96

Then, the conditional knockout male mice were bred with CAG-*cre* transgenic female mice that retained Cre recombinase activity in oocytes (Sakai and Miyazaki, 1997), thereby producing $Kid^{+/-}$ offspring (Figure 1A). The success of these procedures was confirmed by Southern blotting and PCR analyses (Figures 1B–1D and data not shown). We used F1-F3 hybrid offspring from these $Kid^{+/-}$ intercrosses (C57BL/6 × 129/Sv mixed background) for the analyses, unless otherwise noted.

Genotype analysis of more than 300 live-born mice revealed that $Kid^{+/-}$ intercrosses yielded $Kid^{+/+}$: $^{+/-}$: $^{-/-}$ offspring at ratio of approximately 1:2:0.5, suggesting that about 50% of $Kid^{-/-}$ embryos died (Table 1). By analyzing the embryos from $Kid^{+/-}$ intercrosses, we found that about half of the $Kid^{-/-}$ embryos died prior to E9.5 (Table 1). We also showed that $Kid^{-/-}$ x $Kid^{+/-}$ crosses yielded $Kid^{-/-}$ offspring, although the number was less than 50% of that expected (Table 1). Moreover, even $kid^{-/-}$ intercrosses yielded healthy offspring for at least four generations. After backcrossing to a C57BL/6 genetic background for eight generations, the $Kid^{-/-}$ mice showed a more severe phenotype than those in the mixed background (Table 1). Nevertheless, the surviving $Kid^{-/-}$ embryos developed into healthy, fertile adult mice (Table 1).

We confirmed the lack of Kid expression in E14.5 $Kid^{-/-}$ mouse embryonic fibroblasts (MEFs) (Figure 1E). The absence of Kid did not affect the growth rate of MEFs (Figure 1F). Immunofluorescent analysis revealed that a subpopulation of $Kid^{-/-}$ MEFs showed similar mitotic phenotypes as Kid-depleted HeLa cells (data not shown). It may be worthy to mention that comparable numbers of meta II-arrested oocytes with similar morphology were ovulated from $Kid^{-/-}$ and $Kid^{+/+}$ females following superovulation treatment (Figures 1G and 1H). No histological abnormality was found in the $Kid^{-/-}$ testis either, and the motility of the sperms of $Kid^{-/-}$ male mice was normal, as assessed by light microscopy (data not shown).

All these results indicate that Kid is specifically critical for early embryogenesis in mice, but not essential for somatic cell mitosis or meiosis.

Kid Deficiency Results in Fragmentation of the Female Pronuclei and Nuclei in Early Blastomeres

To examine how Kid is involved in early embryogenesis, we obtained 1-cell-stage embryos from the oviducts, cultured them in vitro, and analyzed them for Kid expression. Immunofluorescent staining showed that Kid was clearly detected in both male and female pronuclei in $Kid^{+/+}$1-cell-stage embryos (Figure 2A). However, after nuclear envelope breakdown (NEBD), Kid did not

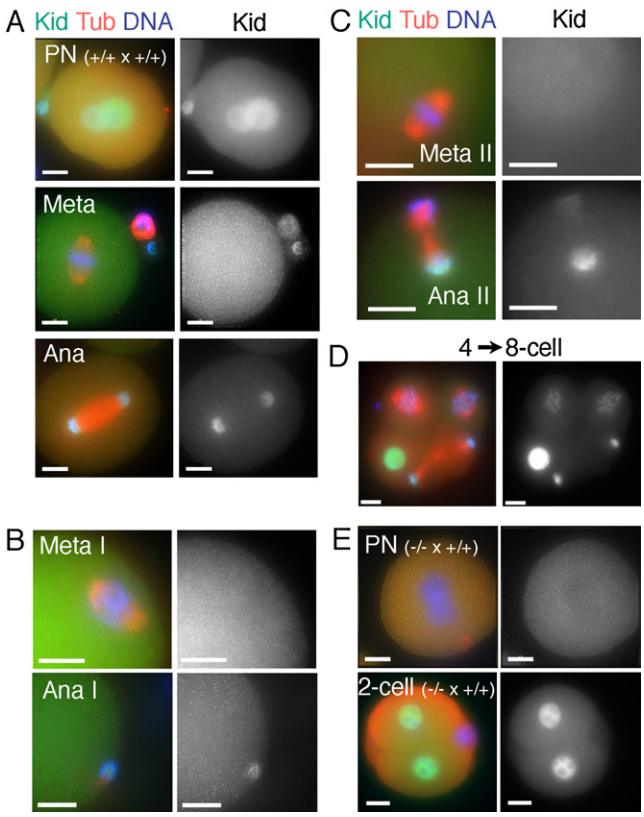

Figure 2. Expression and Localization of Kid in Early-Stage Embryos
Immunostaining of early-stage embryos for Kid, β-tubulin and DNA.
(A) 1-cell/pronuclear stage (PN), metaphase (Meta) and anaphase (Ana) of the first mitosis of $Kid^{+/+}$ embryo.
(B and C) Metaphase and anaphase of wild-type oocyte meiosis I (B) and II (C). Only half of the Ana I spindle was shown.
(D) $Kid^{+/+}$ embryo undergoing the third mitosis.
(E) Pronuclear stage (PN) and 2-cell-stage $Kid^{+/-}$ embryos derived from $Kid^{-/-}$ female x $Kid^{+/+}$ male.
Scale bars represent 15 μm.

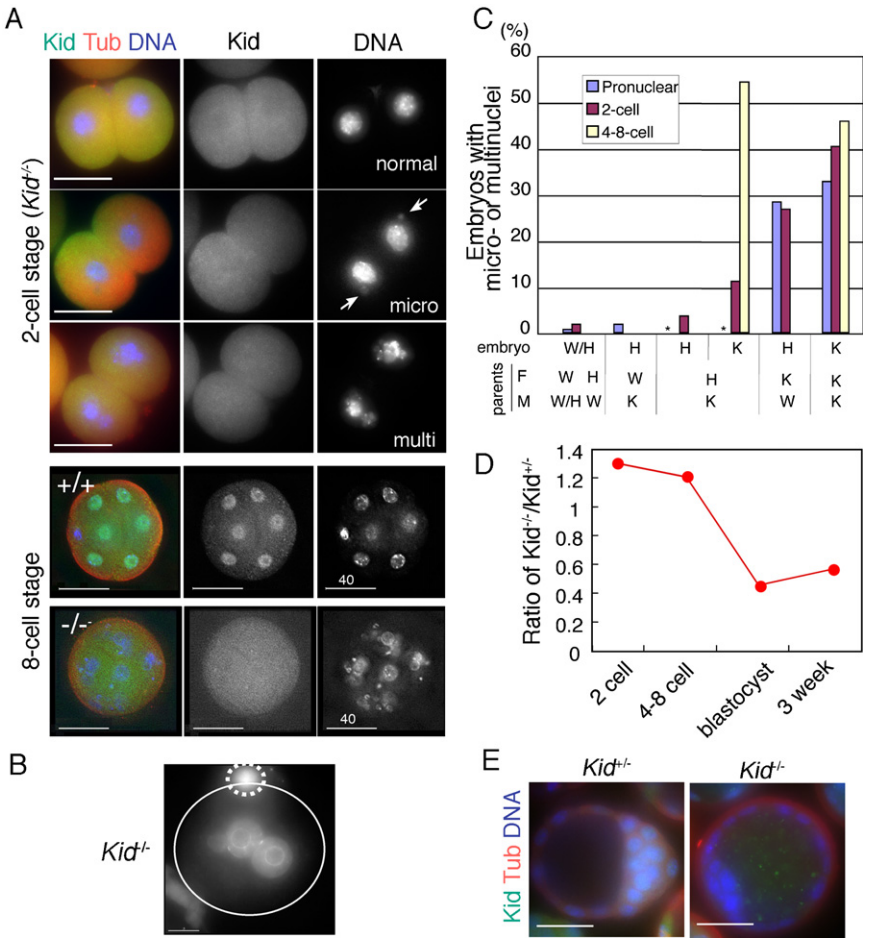

Figure 3. Kid Deficiency Causes Formation of Multinuclei in Early-Stage Embryos

(A) Immunostaining of 2-cell- or 8-cell-stage embryos derived from $Kid^{+/+}$ or $Kid^{-/-}$ intercrosses for Kid, β-tubulin and DNA.

(B) Hoechst staining of pronuclear-stage $Kid^{-/-}$ embryo. Line and dashed line outline the cell surface and polar body, respectively.

(C) Percentage of the embryos containing multinucleated pronuclei or blastomeres. Genotypes of the parents and embryos are indicated: W, $Kid^{+/+}$; H, $Kid^{+/-}$; K, $Kid^{-/-}$. Pronuclear-stage embryo derived from $Kid^{+/-}$ female was not evaluated (asterisk).

(D) Ratio of the number of $Kid^{+/-}$ to $Kid^{-/-}$ at indicated stages derived from $Kid^{+/-}$ female × $Kid^{-/-}$ male. The exact numbers for (C) and (D) are shown in Table 1 and Table S1.

(E) Immunostaining of $Kid^{+/-}$ or $Kid^{-/-}$ blastocyst-stage (E3.5) embryo collected from the oviduct of a $Kid^{+/-}$ female that had been mated with a $Kid^{-/-}$ male.

Scale bars represent 40 μm.

accumulate effectively on the chromosomes and appeared to present diffusely throughout the cytoplasm during prometaphase and metaphase, while at anaphase Kid was strongly detected on the chromosomes (Figure 2A). The same was true for the second mitosis (the mitosis from the 2-cell to 4-cell stage, data not shown) and the first and second meiosis of oocytes (Figures 2B and 2C). In contrast, at the third (the mitosis from the 4-cell to 8-cell stage) and later mitosis, chromosomal accumulation of Kid was clearly detected at prometaphase and metaphase (Figure 2D), just as that were during somatic cell mitosis (Tokai et al., 1996, see also Figure 5A). Time-lapse observations of exogenously introduced EGFP-Kid also showed less efficient localization to metaphase chromosomes in the first mitosis than in somatic mitosis (Figure S1 available online). These results suggest that, although it is not clear whether Kid functions on the prometaphase/metaphase chromosomes and spindles or not, Kid may play a role in the oocyte and early-stage embryos by localizing on the anaphase/telophase chromosomes.

While the Kid signal was absent in the pronuclei of $Kid^{+/-}$ 1-cell-stage embryos derived from $Kid^{-/-}$ female x $Kid^{+/+}$ male, those embryos expressed a detectable level of Kid at the 2-cell stage (Figure 2E), indicating that zygotic expression of Kid began as early as the 2-cell stage. Taking advantage of this, we next performed genotype analysis by immunofluorescent staining with anti-Kid antibody of 2- to 8-cell-stage embryos produced from $Kid^{+/-}$ x $Kid^{-/-}$ crosses. The data revealed that $Kid^{-/-}$ embryos were produced at the expected Mendelian frequency (Table 1), indicating that Kid deficiency did not affect the fertilization. However, Hoechst staining of these embryos revealed that Kid deficiency caused micro- or multinucleated blastomeres at high frequency (Figures 3A and 3C and Table S1). More surprisingly, about 30% of 1-cell-stage embryos derived from $Kid^{-/-}$ female mice contained more than three (in most cases more than four) pronuclei with variable size (Figures 3B and 3C; see also Figure 4A). Multipronucleated $Kid^{-/-}$ 1-cell-stage embryos had both first and second polar bodies (data not shown). In addition, a multipronucleated phenotype was rarely observed in the zygotes derived from $Kid^{+/+}$ females mated with $Kid^{-/-}$ males (Figure 3C). These results indicate that multipronuclei did not result from polyspermy or failure of polar body extrusion, but from the malformation of the female pronuclei.

We next examined the blastocyst-stage embryos collected at E3.5 from the oviducts of $Kid^{+/-}$ female mice that had been crossed to $Kid^{-/-}$ males. The number of $Kid^{-/-}$ blastocysts was only about 50% of the expected number (Table 1 and Figure 3D). However, the surviving $Kid^{-/-}$ blastocysts were normal in size, appearance, and nuclear morphology (Figure 3E). These data suggested that 4- to 8-cell-stage embryos with malformed nuclear blastomeres stopped dividing or died before the blastocyst stage.

Lack of Anaphase Chromosome Compaction in the Absence of Kid Is Relevant to the Formation of Multinucleated Cells

How are micro- and multinuclei formed in Kid-deficient embryos? And why are such abnormalities found in part but

not all of the Kid-deficient early embryos? To address these questions, we performed time-lapse confocal microscopic imaging of chromosomes during the first or second mitosis. Chromosomes were visualized by injection of capped-mRNA encoding the EGFP-tagged methyl-CpG binding domain of MBD1 fused with a nuclear localization signal (EGFP-MBD-NLS) in pronuclear-stage zygotes (Yamagata et al., 2005). Both $Kid^{+/+}$ and $Kid^{-/-}$ 1-cell-stage embryos underwent NEBD between 28–30 hr after human chorionic gonadotrophin (hCG) injection, indicating that neither Kid deficiency nor expression of EGFP-MDB-NLS caused an obvious delay prior to the onset of the first mitosis (Nagy et al., 2003).

After NEBD, even when 1-cell-stage $Kid^{-/-}$ embryos contained multiple pronuclei, all the chromosomes congressed to a single metaphase plate (Figure 4A and Movie S1). $Kid^{-/-}$ zygotes showed no prometaphase/metaphase delay (Figure 4B) and formed a metaphase spindle with aligned chromosomes, which was indistinguishable from that in $Kid^{+/+}$ zygotes (Figure 4C). These results, together with our observation that obvious accumulation of Kid was not detected on the prometaphase/metaphase mitotic apparatus of the oocyte meiosis or the first two mitoses (Figure 2), strongly suggested that Kid deficiency did not cause an abnormality in spindle formation or metaphase chromosome alignment in oocyte meiosis or early embryonic division.

Upon anaphase onset, in $Kid^{+/+}$ zygotes, the length of the chromosome mass along the pole-to-pole axis was slightly increased during the poleward migration of the chromosomes mass. Then, just after the poleward migration of the pole-proximal edge of the chromosome mass ceased (around 25 min post anaphase onset; red bar in Figure 4E) and just before nuclear expansion began, the length of the chromosome mass decreased to a minimum (Figures 4D and 4E and Figure S2). In contrast, in $Kid^{-/-}$ zygote, although the pole-proximal edge of the anaphase chromosome mass moved with equivalent kinetics to those in $Kid^{+/+}$ zygotes, the length of the chromosome mass was continuously increased even after poleward movement ceased. Then, NE reassembly began without obvious compaction of the chromosome mass (Figures 4D and 4E and Figure S1). These observations were also confirmed by analyzing the chromosome-occupied area in the z-stacked images from the onset of anaphase untill the completion of nuclear expansion during G1 phase. In $Kid^{+/+}$ zygotes, the chromosome-occupied area showed a transient decrease to the lowest level just before the nuclear expansion (Figure 4F). Such a decrease was not detected in $Kid^{-/-}$ zygotes (Figure 4F). In $Kid^{-/-}$ embryos, a single or several chromosomes were often apart from the main chromosome mass at late anaphase and formed small independent nuclei, resulting in micro- or multinucleated blastomeres (12/28 of the first mitoses) (Figures 4G and 4H and Movies S2 and S3). These results strongly suggest that the less tightly compacted anaphase/telophase chromosome mass caused the formation of micro- or multinucleated cells in $Kid^{-/-}$ embryos. In time-lapse imaging experiments, we observed lagging chromosomes in even $Kid^{+/+}$ embryos at certain frequency (observed in 5 out of 18 embryos) at early anaphase of the first mitosis. Because we rarely observed micronuclei in wild-type 2-cell-stage embryos that had been cultured in vitro without live-imaging (Figure 3C and Table S1), this was likely resulted from the live-imaging system.

Time-lapse imaging of chromosomes in $Kid^{-/-}$ zygotes also demonstrated that the multinucleated phenotype at the 1-cell stage was restored in the metaphase of the first mitosis, but induced again in the subsequent anaphase/telophase with a particular frequency if Kid was still absent (Figures 4A and Movie S1). Indeed, among $Kid^{-/-}$ embryos derived from $Kid^{-/-}$ intercrosses, the percentage of multinucleated embryos was about 40% and was not significantly changed from the 1- to 8-cell stage (Figure 3C and Table S1). In contrast, although 25%–30% of 1- or 2-cell-stage $Kid^{+/-}$ embryos derived from $Kid^{-/-}$ female x $Kid^{+/+}$ male crosses exhibited the multinucleated phenotype, all 4- to 8-cell-stage embryos from the same cross showed normal nuclear morphology (Figure 3C and Table S1). It is likely that in these $Kid^{+/-}$ embryos, zygotic expression of Kid in 2-cell-stage embryos restore the multinucleated phenotype during the second mitosis.

Furthermore, we observed that only about 10% of $Kid^{-/-}$ 2-cell-stage embryos derived from $Kid^{+/-}$ female x $Kid^{-/-}$ male crosses exhibited a micro- or multinucleated phenotype; however, the percentage of $Kid^{-/-}$ embryos with micro- or multinucleated blastomeres was increased to more than 50% at the 4- to 8-cell stage (Figure 3C and Table S1). The Kid signal was decreased to an undetectable level by the late 2-cell stage in these embryos (data not shown), suggesting that the maternal Kid was exhausted before the onset of the second mitosis, causing the formation of multinucleated blastomeres during the second and/or third mitosis. From these results, we concluded that the process of female pronuclear formation and each of the first two to three mitoses requires Kid for proper pronuclear or daughter nuclear formation. Kid deficiency did not cause a severe abnormality in mitosis during post-morula-stage development, and therefore $Kid^{-/-}$ embryos that happened to pass the 4- to 8-cell-stage without multinucleated blastomeres were able to grow into neonates and then adults (Figure 4I).

Kid Localizes in the Interstices between Anaphase Chromosomes

Next, to address the role of Kid during anaphase and telophase, we first analyzed detailed localization of Kid after anaphase onset by using cultured cells. Kid localized along the entire length of the metaphase chromosomes and spindle microtubules (Figure 5A). Upon metaphase/anaphase transition, Kid signals on the chromosome arms and spindle microtubules became weak and instead, Kid was enriched in the spindle pole-proximal side of the chromosomes, showing a striated signal pattern (Figure 5A). Immunofluorescent confocal microscopic observation revealed that strong Kid signals, along with microtubules, were detected in the interstices between neighboring chromosomes (Figure 5B). Notably, almost no Kid signals were detected along chromosome surfaces that were not in close contact with neighboring chromosomes (Figure 5B).

We next evaluated the relationship between the localization pattern of Kid and the ratio of cell length to width, which roughly reflects the progression of anaphase. In most early anaphase cells (phase I), the Kid signal was found diffusely on the chromosomes (Figure 5A). At mid-anaphase when the ratio of cell length

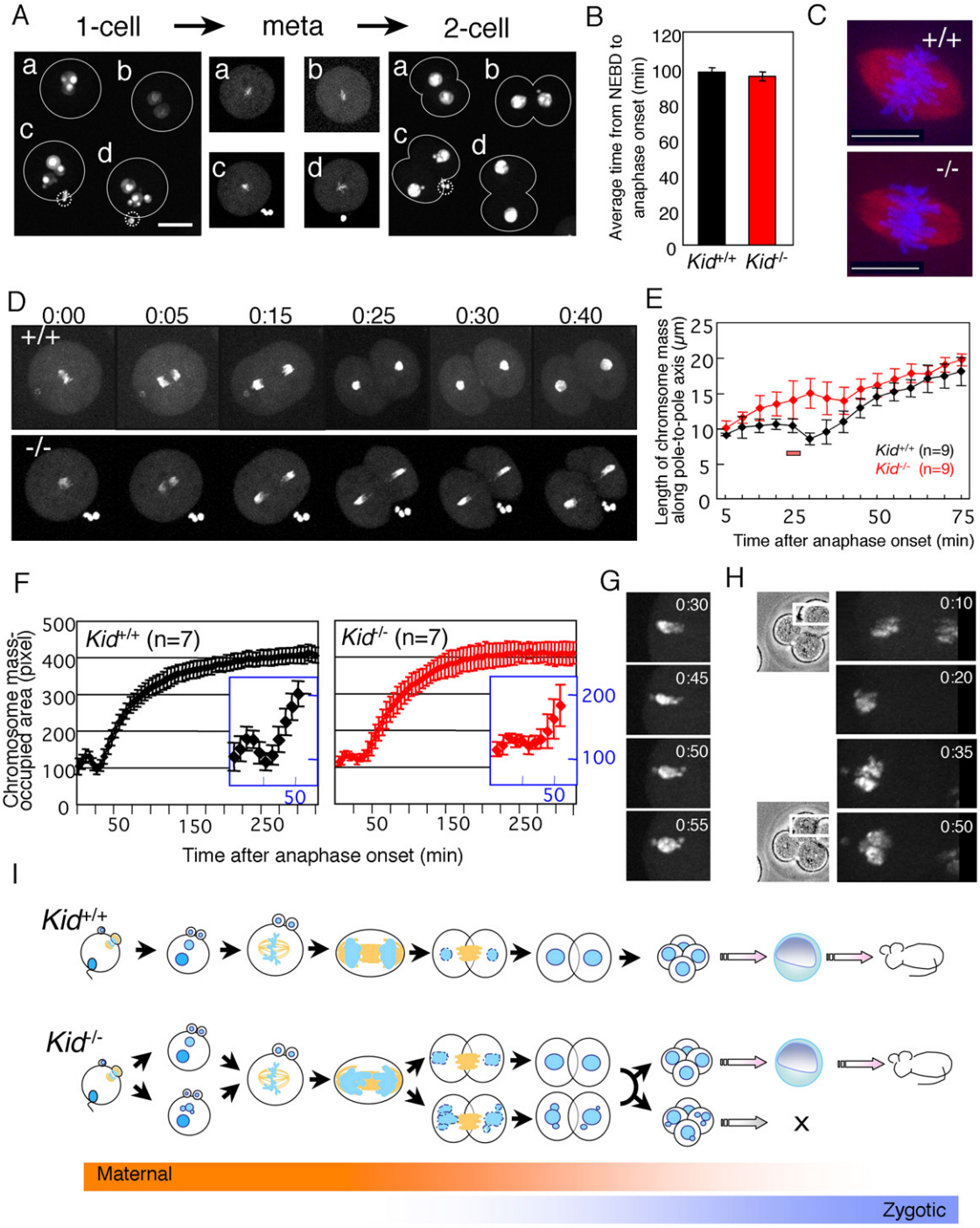

Figure 4. Kid-Mediated Anaphase Chromosome Compaction Prevents Formation of Multinuclei in Early-Stage Embryos

(A) Time-lapse imaging of first mitosis of four (a–d) *Kid*$^{-/-}$ embryos. Chromosomes were visualized using EGFP-MBD-NLS. The first (left; 1-cell stage) and last (right; 2-cell stage) frames of Movie S1, and metaphase of each embryo (middle) are shown. Line and dashed line outline the cell surface and polar body, respectively. Embryos c and d contain multipronuclei at 1-cell stage and embryos b and c contain micronuclei at 2-cell stage.

(B) The average time from NEBD to the onset of anaphase during the first mitoses of *Kid*$^{+/+}$ and *Kid*$^{-/-}$ embryos. Ten embryos were examined for each genotype. Error bars represent SEM.

(C) Confocal fluorescence imaging of metaphase spindle (red; β-tubulin) and chromosomes (blue; PI) of the first mitosis of *Kid*$^{+/+}$ and *Kid*$^{-/-}$. Scale bars represent 15 μm.

(D) Time-lapse imaging of first mitosis of *Kid*$^{+/+}$ and *Kid*$^{-/-}$ embryos. Chromosomes were visualized with EGFP-MBD-NLS and fluorescent images were acquired at 5 min intervals. The last frame of metaphase is labeled as 0 min (time in hr:min).

to width became greater than 1.3 (phase II), more than 80% of the cells showed the characteristic striated pattern of Kid signals (Figure 5D). In all the late anaphase to early telophase cells with an ingressing cleavage furrow (phase III), Kid signals exhibited the striated pattern (Figures 5C and 5D). Part of the phase III cells exhibited no obvious lamin A/C signals around chromosomes, indicating that accumulation of Kid between chromosomes was established before NE reassembly began and Kid remained there throughout the NE reassembly process (Figure 5C). When chromosomes were decondensed, Kid was uniformly distributed in the daughter nuclei (Figure 5C). Immunoelectron microscopic observations of phase III HeLa cell further revealed that even when adjacent chromosomes tightly adhered to each other without an interstice, Kid signals were retained at the boundary of adjacent chromosomes (Figure 5E). Consistent with the findings of immunofluorescent microscopy (Figure 5B), no Kid signals were found on the chromosome surfaces that were not faced to neighboring chromosomes (Figure 5E). Accumulation of Kid in between telophase chromosomes was also confirmed by immunofluorescent deconvolution images (Figure 5F and Movie S4).

To identify the domain responsible for the unique localization of Kid during anaphase and early telophase, we constructed GFP-tagged Kid mutants lacking the DNA binding domain (GFP-Kid-delDB) or motor domain (Kid-delMot) and expressed them at a relatively low level in NIH 3T3 cells by retrovirus infection. Under these conditions, exogenous GFP-Kid shows the same localization pattern as endogenous Kid throughout mitosis (Ohsugi et al., 2003). GFP-Kid-delDB was strictly localized to the microtubules connecting centrosomes and chromosomes, while deletion of the motor domain resulted in the mislocalization of Kid to the entire anaphase chromosomes (Figure 5G). Namely, little enrichment of Kid in between chromosomes was observed. These results indicate that Kid is localized in the interstices between adjacent anaphase chromosomes in a chromosome- and microtubule- binding dependent manner.

Kid Also Contributes to Shortening Chromosomal Mass along the Spindle Axis in HeLa Cells

We next investigated the effects of Kid-depletion on anaphase/telophase chromosome dynamics and daughter nuclear formation. In control anaphase cells, the kinetochores stained with anti-centromere antiserum (ACA) were localized in a linear array at the pole-proximal edge of the migrating chromosome mass (Figure 6A). In contrast, ACA signals were widely scattered along the spindle axis and the chromosome mass appeared less compacted in Kid-depleted anaphase cells (Figure 6A). To analyze the change of the spatial distribution of kinetochores and the chromosome mass during anaphase and early telophase, we collected a z-series of serial optical sections of cells in phases I-III and stacked them to produce an image depicting all the chromosomes present. Then we measured the length of the ACA-positive area along the pole-to-pole axis (a in Figure 6B) as well as the length and width of the chromosome mass (b and c in Figure 6B). At early anaphase (phase I), kinetochores were distributed within a relatively large area in both control and Kid-depleted cells. Thereafter, in control cells kinetochores became aligned within a narrow area by mid-anaphase (phase II), whereas in Kid-depleted cells kinetochores remained scattered throughout anaphase (Figure 6Ca). Consistent with this, in control cells the length of the chromosome mass along the pole-to-pole drastically decreased at phase II, whereas that in Kid-depleted cells remained long (Figure 6Cb). In both control and Kid-depleted cells, the width of the chromosome mass gradually decreased as anaphase progressed (Figure 6Cc). These results suggest that the rapid alignment of the kinetochores of the segregating chromosomes during anaphase is impaired in Kid-depleted cells. Therefore, Kid likely plays a role in holding individual chromosomes together during the segregation.

Immunofluorescent staining showed that in most Kid-depleted telophase cells, the chromosomes remained distinguishable. In these cells, Lamin A/C was reassembled on the chromosome surface facing the inter-chromosomal gaps, as if decorating the individual chromosomes, resulting in markedly uneven morphology of daughter cell nuclei with many corrugations (Figure 6D). In Kid-depleted cells that had passed through mitosis, 86.0 ± 1.7% of nuclei showed wrinkled or rugose nuclear lamina, while only 12.8 ± 0.6% of control cells had such a wrinkled lamina (average of three independent experiments ± SEM n > 300 in each experiment) (Figure 6E). All these data suggest that in HeLa cells Kid also contributes to anaphase/telophase chromosome compaction by shortening anaphase chromosome mass along the pole-to-pole axis, and thereby ensuring the reassembly of the smooth NE around the entire chromosome mass (Figure 6F).

Taken together, we concluded that loss of Kid causes less efficient compaction of the anaphase/telophase chromosome mass both in somatic and emryonic cell divison, and leads to multinuclear formation specifically at very early embyonic stages.

(E) Average length of chromosome mass along the pole-to-pole axis at the indicated time points after anaphase onset of the first mitosis of $Kid^{+/+}$ and $Kid^{-/-}$. Red bar represents the timing at which poleward migration of the chromosome mass ceased. Error bars represent SEM. n, number of chromosome segments analyzed. Independent data from each chromosome segment are shown in Figure S1.

(F) Average chromosome-occupied area at the indicated time points after anaphase onset of the first mitosis of $Kid^{+/+}$ and $Kid^{-/-}$. Error bars represent SEM. n, number of chromosome segments analyzed. The inset shows an enlargement of time range up to 55 min.

(G and H) Time-lapse imaging of the chromosome from anaphase to telophase of the first (G) or second (H) mitosis of $Kid^{-/-}$ embryo. Time after anaphase onset is indicated (hr:min). Light microscopic images of embryos at 0:10 and 0:50 are also shown in (H) with the white rectangle representing the region of fluorescent images.

(I) Schematic representation of the proposed phenotype and fates of the $Kid^{-/-}$ embryos. The anaphase of meiosis II of the $Kid^{-/-}$ zygote results in multifemale pronuclear formation at high frequency, which is once restored by the metaphase of the first mitosis. In $Kid^{-/-}$ embryos, anaphase chromosomes are less compacted, leading to the formation of multinucleated cells at high frequency again. A similar situation occurs at the second, but not at the third or later mitosis. Multinucleated phenotype at 4-cell stage is no longer restored by the next mitosis, and leads to growth arrest or death. Orange and blue bars schematically represent the amount of maternal and zygotic transcripts, respectively.

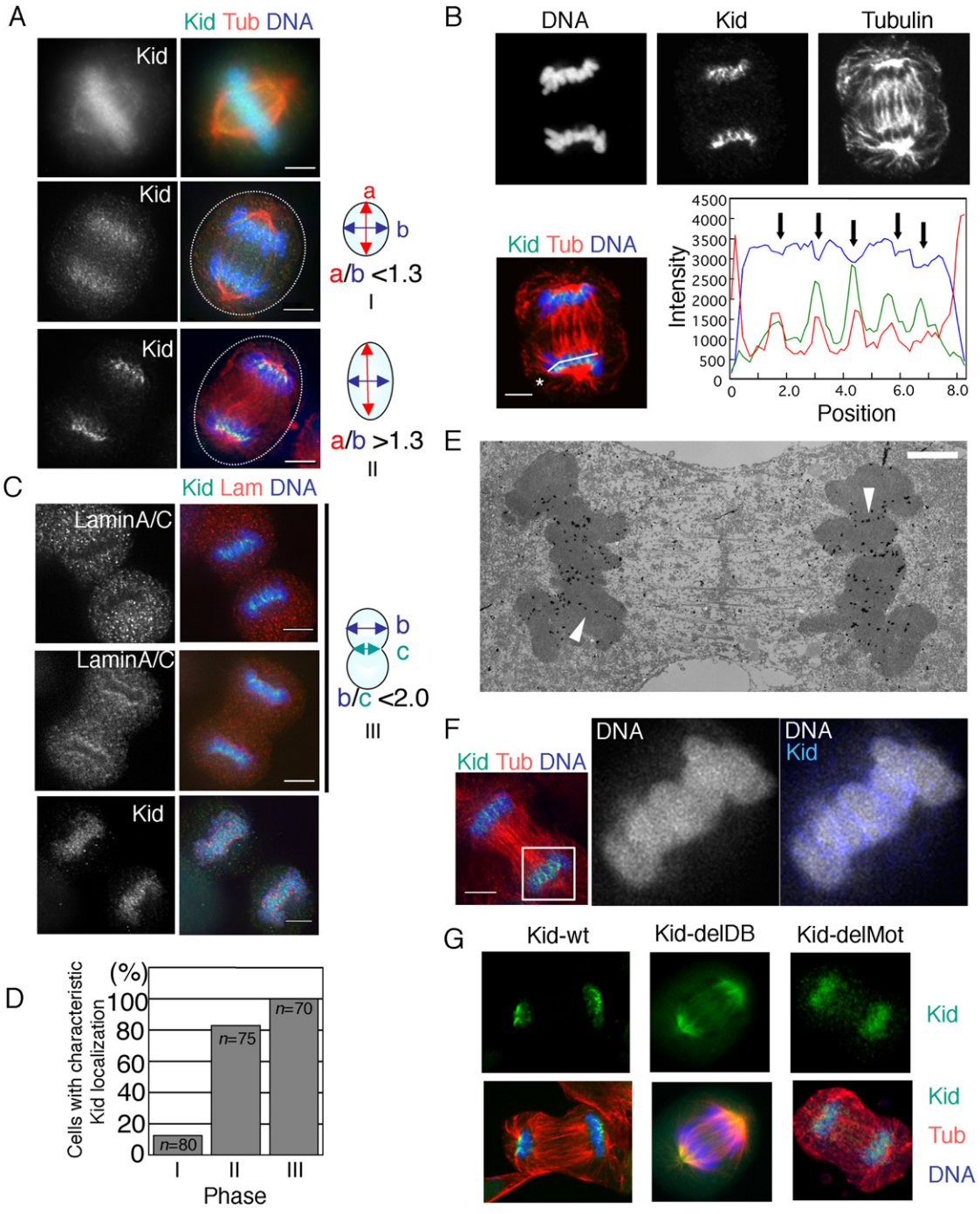

Figure 5. Kid Localizes in the Interstices between Anaphase Chromosomes

(A) Immunostaining of metaphase and anaphase HeLa cells for Kid, DNA and α-tubulin. Dashed lines outline the cell surface. Phases I and II are defined by cells having a ratio of cell length (pole-to-pole axis; a) to width (b) less and greater than 1.3, respectively.

(B) A confocal microscopic section of a phase II anaphase HeLa cell stained for Kid, DNA and α-tubulin. The graph shows the intensity of each signal along the white line starting from the asterisk in the merged image. The arrows indicate the positions of chromosome boundaries.

(C) Immunostaining of late anaphase and telophase HeLa cells for Kid, DNA and lamin A/C. Phase III is defined by cells having an ingressing cleavage furrow and a ratio of cell width at the widest (b) relative to that at the narrowest (c) region of less than 2.0.

(D) Proportion of cells with striated patterns of Kid signal in phase I-III cells. n, number of cells examined. (E) Immunoelectron microscopic observation of Kid in phase III HeLa cell. The arrowheads indicate the Kid signals along the chromosome boundaries. Scale bar represents 2 μm.

(F) A deconvolution image of phase III HeLa cells stained for Kid, DNA and α-tubulin. Magnified images from the area within the white rectangle in the left panel are shown for chromosomes alone and chromosomes plus Kid. See also Movie S4.

DISCUSSION

For faithful daughter nuclear formation, all the chromosomes need to be close together, forming a compact cluster, before NE reassembly begins. Emerging evidence has revealed the importance of the maintenance of anaphase chromosome condensation and axial compaction of the anaphase chromosome arms to achieve this (Mora-Bermudez et al., 2007; Vagnarelli et al., 2006). The present study demonstrates that the chromokinesin Kid contributes to this event by shortening anaphase chromosome mass in both HeLa cells and mouse zygotes. Previous studies demonstrated that depletion of Kid from HeLa cells, in which Kid localizes to the prometaphase/metaphase chromosome arms and spindles, results in prometaphase delay accompanied with defects in chromosome arm alignment and metaphase spindle size (Tokai-Nishizumi et al., 2005; Zhu et al., 2005). Therefore, these pre-anaphase defects might be in part relevant to the anaphase phenotype observed in Kid-depleted HeLa cells. Nonetheless, our data show that in mouse embryos, pre-anaphase processes appear unaffected in Kid$^{-/-}$ embryos. These data strongly suggest that the formation of multinucleated cells during the early embryonic stage is due to the loss of Kid function during anaphase and telophase, but not prometaphase and metaphase.

The mechanism by which Kid promotes compaction of the anaphase/telophase chromosome mass along the spindle axis is not known; however, the characteristic localization of Kid during anaphase and telophase must be an important clue. We show that, during anaphase, Kid is colocalized with microtubules in between adjacent chromosomes and that both the motor domain and DNA-binding domain are critical for Kid localization (Figure 5G). These data suggest that a subset of anaphase microtubules located between anaphase chromosomes plays a role in proper chromosome segregation by recruiting Kid (Figure 6F). At prometaphase and metaphase, Cdc2/cyclin B-mediated Kid phosphorylation of Thr463 downregulates Kid's affinity for microtubules, allowing Kid to localize on chromosomes (Ohsugi et al., 2003; Shiroguchi et al., 2003). At anaphase/telophase, Thr463 of Kid is no longer phosphorylated, and therefore Kid shows high affinity for microtubules. This suggests that increased microtubule-binding activity of Kid, together with its DNA-binding activity, contributes to its localization at anaphase. Indeed, FRAP (fluorescence recovery after photobleaching) assay revealed that while at prometaphase/metaphase the fluorescence of exogenously expressed EGFP-Kid on chromosomes recovers within seconds, recovery of fluorescence at anaphase is almost undetectable within one minute, (our unpublished results), suggesting that Kid binds to microtubules and/or chromosomes very tightly during anaphase. Taken together, Kid would mediate the axial shortening of chromosome arms (Mora-Bermudez et al., 2007) by acting as a DNA-bound microtubule motor protein. Further experimental verification will help establish the precise molecular mechanism of Kid-mediated anaphase chromosome compaction.

Why does Kid deficiency result in micro- or the formation of multinucleated cells only in very early-stage embryos? In mice, a burst of zygotic gene expression begins at the 2-cell stage (Flach et al., 1982), which is accompanied by the degradation of maternal factors (Bachvarova and De Leon, 1980). Therefore, it appears that the embryonic stages severely affected by Kid deficiency are those during which NE reassembly occurs under the significant influence of the ooplasm. It is theoretically possible that other molecules or mechanism might function after the 4- to 8-cell stage to complement Kid or even render its function in anaphase chromosome function redundant. However, it is important to note that Kid itself behaves differently in these early cell divisions with respect to its chromosomal localization at prometaphase and metaphase (Figure 2). Therefore, it is likely that the mitotic process is regulated in a specialized manner during these "maternally controlled" meioses and mitoses. We speculate that in mouse zygotes and early embryonic blastomeres, the cytoplasm and/or anaphase chromosomes possess strong ability to assemble the NE compared to those in somatic cells, and therefore, in the absence of Kid, micro- or multinuclei are readily formed. Indeed, the small GTP protein Ran, which promotes NE reassembly (Bamba et al., 2002; Zhang and Clarke, 2000, 2001), is predominantly associated with chromosomes in mouse oocytes, but to a lesser degree in HeLa cells (Hinkle et al., 2002). It is interesting to note that in *Xenopus* egg extracts, Xkid is not associated with anaphase chromosomes (Funabiki and Murray, 2000) and during *Xenopus* cleavage divisions, anaphase chromosomes do not have to be tightly gathered as NEs are reassembled around individual chromosomes to form micronuclei-like structures called karyomeres (Lemaitre et al., 1998; Montag et al., 1988). In contrast, when cells begin to undergo zygotic expression-dependent somatic mitosis after midblastula transition (Lemaitre et al., 1998), karyomere formation ceases and Xkid is apparently localized on anaphase/telophase chromosomes during somatic mitosis (Antonio et al., 2000).

Although Kid is critically important for "maternally controlled" divisions, the formation of multinucleated cells caused by Kid deficiency does not lead to cell cycle arrest at the 1- to 4-cell stage, but results in embryonic death during the morula stage (Figure 3D). Because NE and nuclear architecture are important for gene regulation (Akhtar and Gasser, 2007), we speculate that the formation of multinucleated cells may disturb the proper zygotic gene expression, leading to embryonic death.

The presence of multinucleated blastomeres in human early-stage embryos is a crucial parameter for judging the suitability of embryos for intrauterine transfer in assisted reproductive technologies. Multinucleated blastomeres are often observed in human embryos produced by in vitro fertilization or intracytoplasmic sperm injection, and the molecular mechanisms or factors influencing nuclear formation in early embryos remain poorly understood (Munne and Cohen, 1998). Our studies shed light on the importance of anaphase chromosome compaction to prevent mammalian early embryos from forming multinucleated blastomeres.

(G) Confocal fluorescence imaging of GFP-Kid-wt, GFP-Kid-delDB, and GFP-Kid-delMot expressed at low level in NIH 3T3 cells. Cells were stained for GFP, DNA, and α-tubulin.

Scale bars in panels except for (E) represent 5 μm.

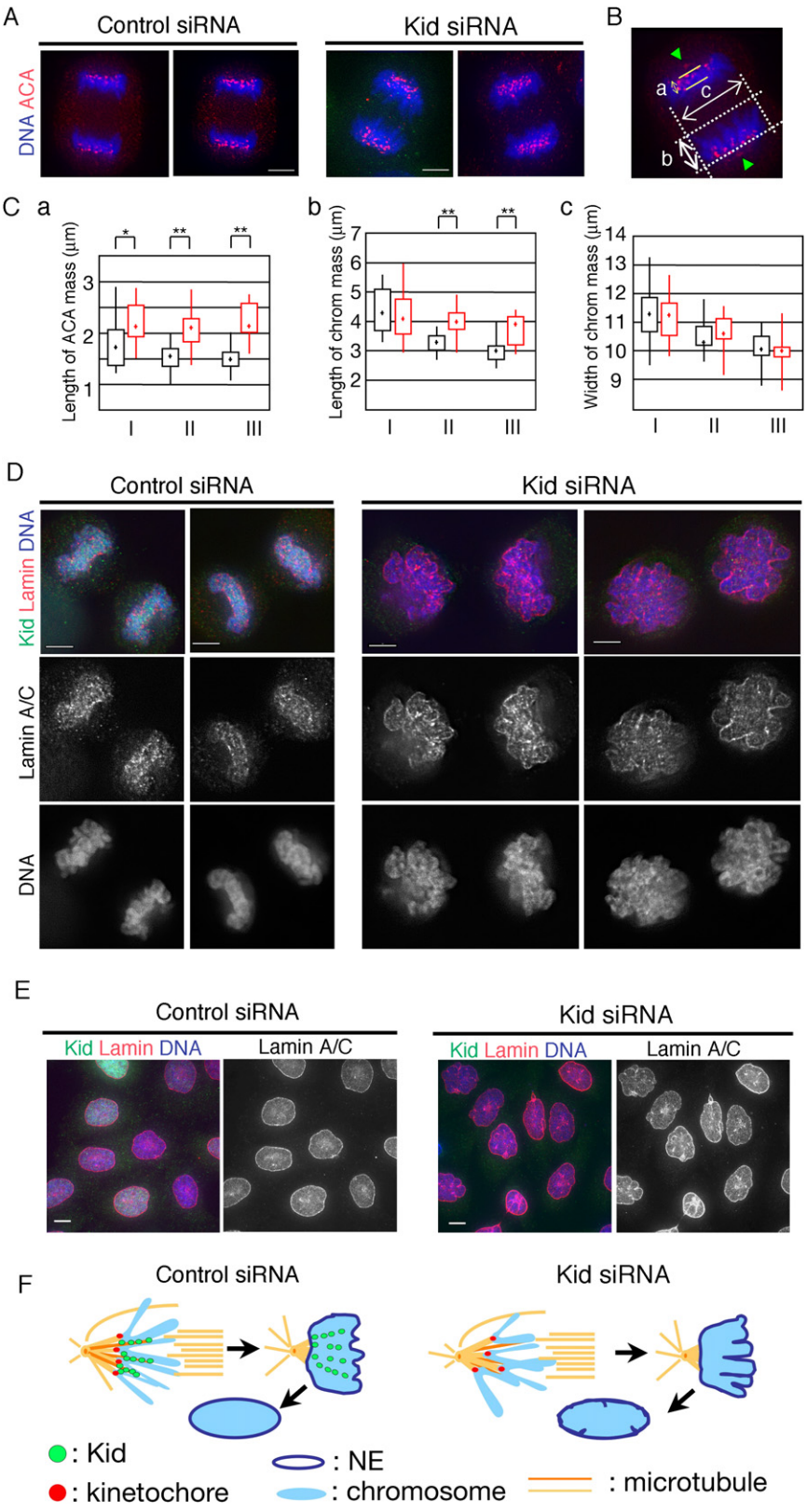

Figure 6. Kid Contributes to the Axial Shortening of Anaphase Chromosome Mass and the Formation of Daughter Nuclei with Smooth Surfaces

(A and B) Control or Kid-RNAi anaphase HeLa cells were stained for Kid, DNA, and kinetochores (ACA). γ-tubulin was also stained in (B). The arrowheads in (B) indicate the centrosomes. The arrows a-c in (B) indicate the lengths measured in (C).

(C) Length of ACA-positive area (a), length of chromosome mass (b), and width of chromosome mass (c) of control (black) or Kid-RNAi (red) HeLa cells at phase I-III represented as whisker plots. The bottom and top of the box show lower and upper quartile values, respectively. The median is indicated with "+" and whiskers denote the range. *$p = 0.027$ and **$p < 0.001$ (The Mann-Whitney U-test). Thirteen-22 cells were examined in each category.

(D and E) Immunostaining of control or Kid-RNAi telophase (D) or interphase (E) HeLa cells for Kid, DNA and lamin A/C. Cells were fixed at 10 hr (D) or 24 hr (E) after the release from thymidine block.

(F) Schematic representation showing the localization and role of anaphase/telophase Kid. Kid localizes in the interstices between anaphase chromosomes along the microtubules located there (shown as dark orange lines). In the absence of Kid, lateral adherence of anaphase chromosomes is impaired, resulting in malalignment of anaphase chromosomes, NE reassembly in the boundaries between chromosomes, and rugose nuclear lamina formation.

Scale bars represent 5 μm.

EXPERIMENTAL PROCEDURES

Generation of Kid-Deficient Mice

See Supplemental Data for description of the generation of Kid-deficient mice. Experiments with animals were carried out in accordance with the guidelines for animal use issued by the Committee of Animal Experiments, Institute of Medical Science, University of Tokyo.

Collection and Culture of Oocytes and Early-Stage Embryos

Female mice (8–12 weeks old) were superovulated by intraperitoneal injections of pregnant mare serum gonadotropin (PMSG) and human chorionic gonadotrophin (hCG) at 46–48 hr intervals. Sixteen to eighteen hours after hCG injection, zygotes were collected from the ampulla region of the oviducts of plug-positive females, treated with hyaluronidase to remove cumulus cells, and cultured in drop of M16 medium covered with mineral oil (Sigma) at 37°C under 5% CO_2 for 8–10 hr for pronuclear stage, 12–18 hr for the first mitosis, 24–28 hr for 2-cell stage, or 36–40 hr for 4- to 8-cell stage. Meta II arrested oocytes were collected from females that had not been mated with males. For analysis of meiosis I, oocytes with germinal vesicles were isolated by disaggregating ovaries from females treated with PMSG for 48 hr in M2 medium and cultured in M16 medium for 9–10 hr before fixation. Blastocyst-stage embryos were collected at E3.5 by flushing the oviducts.

Time-Lapse Live Microscopy

The expression plasmid for EGFP-MBD-NLS [pcDNA3.1EGFP-MBD-NLS polyA(83)] was a gift from K. Yamagata, and in vitro mRNA transcription was performed as described previously (Yamagata et al., 2005). For EGFP-Kid expression, cDNA encoding MBD-NLS was replaced by that of hKid. A few picoliters of 50 ng/μl (EGFP-MBD-NLS) or 100 ng/μl (EGFP-Kid) denatured mRNA was microinjected into pronuclear-stage zygotes as described previously (Adachi et al., 2007) and the zygotes were cultured in a drop of M16 medium covered with mineral oil at 37°C under 5% CO_2 until the observation was started. Embryos were transferred to a drop of M16 medium covered with mineral oil in a glass-bottomed dish and observed with a laser spinning disk live-cell confocal microscopy system utilizing a Yokogawa CSU22 controlled by Metamorph software (Universal Imaging), equipped with a CO_2 microscope stage incubator. Z-series of 18–23 sections in 2.5 μm increments were captured every 5 min and projected onto a single image plane. Quantification of chromosome-occupied area was performed using MetaMorph Software. In the experiments shown in Figures 6E and 6F, embryos whose pole-to-pole axis were parallel to the focal plane were selected for analysis. In the experiments shown in Figure S1A, pcDNA3.1EGFP-Kid plasmid was transfected into NIH 3T3 cells.

Cell Culture, Retrovirus Infection, and RNA Interference

HeLa cells and NIH 3T3 cells were cultured in DMEM with 10% fetal calf serum or calf serum, respectively. Mouse embryonic fibroblasts (MEFs) were obtained from E14.5 embryos by an established procedure (Todaro and Green, 1963) and cultured in DMEM with 10% fetal calf serum and 50 μM β-mercaptoethanol. The growth rates of the MEFs were determined by plating triplicate cultures of 1 x10^5 cells in 60-mm dishes. At 3-day intervals, the total number of cells per culture was determined prior to dilution of the cells for repassage. Retrovirus-mediated expression of Kid in NIH 3T3 cells was performed as described previously (Yoshida et al., 2003). DNA fragments encoding GFP-KiddelDB (amino acids 1-515) and GFP-KiddelMot (amino acids 405-665) were cloned into pMX-puro vector (Onishi et al., 1996) for retrovirus production. RNA interference of Kid was carried out as described previously (Tokai-Nishizumi et al., 2005). HeLa cells were synchronized in S phase by 2.5 mM thymidine block for 20–24 hr when necessary.

Antibodies

For immunoblotting and immunofluorescent staining, antibodies against Kid (polyclonal, Tokai et al., 1996), α-tubulin, β-tubulin, γ-tubulin (monoclonal, Sigma), or lamin A/C (monoclonal, Santacruz) were used. For kinetochore staining, anti-centromere antiserum (ACA, gift of Y. Takasaki) was used.

Immunofluorescence Microscopy

Cells were grown on a glass coverslip, fixed and stained as described previously (Ohsugi et al., 2003). In the experiments shown in Figures 6A–6C, cells were stained for Kid and centrosomes in addition to chromosomes and kinetochores, confirming that the residual Kid was at undetectable level and that both centrosomes were in a single focal plane. Oocytes and early-stage embryos were treated with acidic Tyrode's solution to remove the zona pellucida, washed with 0.5% polyvinyl pyrrolidone/PBS, fixed with 4% paraformaldehyde containing 0.005% Triton X-100 for 30 min at R.T., and then incubated sequentially with the first and secondary antibodies. Unless otherwise specified, image stacks were captured on a microscope controlled by Delta Vision SoftWorx (Applied Precision). When necessary, deconvolution was performed. Image stacks were quick-projected and saved as Photoshop files. Confocal images for Figures 4C, 5B, and 5G were recorded and analyzed with a laser scanning confocal microscope system as follows: Figure 4C: Yokogawa CSU22 controlled by MetaMorph (Universal Imaging), Figure 5B; Fluoview FV1000 controlled by FV10-ASW (Olympus), Figures 5G; Radiance2000 controlled by Lasersharp (Bio-Rad).

Immunoelectron Microscopy

Samples for immunoelectron microscopy were prepared as described (Tokai-Nishizumi et al., 2005). In short, the cells were extracted in PHEM (60 mM PIPES, [pH 6.9, 25] mM HEPES, 10 mM EGTA, 2 mM MgCl2) containing 0.1% Triton X-100 for 1 min at room temperature before fixation with 0.1% glutaraldehyde for 10 min, and incubated with anti-Kid antibody and then with FluoroNanogold (Nanoprobe Inc.). Cells were post-fixed with 2% glutaraldehyde for 15 min, silver enhanced, and processed for electron microscopy as previously described (Tokai-Nishizumi et al., 2005).

SUPPLEMENTAL DATA

Supplemental Data include one table, Supplemental Experimental Procedures, two figures, and four movies and can be found with this article online at http://www.cell.com/cgi/content/full/132/5/771/DC1/.

ACKNOWLEDGMENTS

We thank K. Yamagata and T. Yamazaki for materials and kind advice on immunofluorescence and time-lapse observation of mouse embryos; H. Umemoto for help in genomic cloning; D. Chida for kind advice on manipulating mouse embryos; J. Miyazaki for CAG-*Cre* transgenic mouse; R.F. Whittier, K. Ohsumi, and M. Iwabuchi for helpful discussions; and S. Sugano and M. Watanabe for help in spinning disc confocal microscopy. M.O. and T.Y. were supported by grants-in-aid from the Japan Society for the Promotion of Science and from the Ministry of Education, Culture, Sports, Science, and Technology, Japan. M.O. was also supported by grant from Yamanouchi Foundation for Research on Metabolic Disorders.

Received: September 22, 2007
Revised: November 14, 2007
Accepted: January 17, 2008
Published: March 6, 2008

REFERENCES

Adachi, K., Soeta-Saneyoshi, C., Sagara, H., and Iwakura, Y. (2007). Crucial role of Bysl in mammalian preimplantation development as an integral factor for 40S ribosome biogenesis. Mol. Cell. Biol. *27*, 2202–2214.

Akhtar, A., and Gasser, S.M. (2007). The nuclear envelope and transcriptional control. Nat. Rev. Genet. *8*, 507–517.

Antonio, C., Ferby, I., Wilhelm, H., Jones, M., Karsenti, E., Nebreda, A.R., and Vernos, I. (2000). Xkid, a chromokinesin required for chromosome alignment on the metaphase plate. Cell *102*, 425–435.

Bachvarova, R., and De Leon, V. (1980). Polyadenylated RNA of mouse ova and loss of maternal RNA in early development. Dev. Biol. *74*, 1–8.

Bamba, C., Bobinnec, Y., Fukuda, M., and Nishida, E. (2002). The GTPase Ran regulates chromosome positioning and nuclear envelope assembly in vivo. Curr. Biol. *12*, 503–507.

Burke, B., and Ellenberg, J. (2002). Remodelling the walls of the nucleus. Nat. Rev. Mol. Cell Biol. *3*, 487–497.

Ciemerych, M.A., and Sicinski, P. (2005). Cell cycle in mouse development. Oncogene *24*, 2877–2898.

Clute, P., and Masui, Y. (1997). Microtubule dependence of chromosome cycles in Xenopus laevis blastomeres under the influence of a DNA synthesis inhibitor, aphidicolin. Dev. Biol. *185*, 1–13.

Flach, G., Johnson, M.H., Braude, P.R., Taylor, R.A., and Bolton, V.N. (1982). The transition from maternal to embryonic control in the 2-cell mouse embryo. EMBO J. *1*, 681–686.

Funabiki, H., and Murray, A.W. (2000). The Xenopus chromokinesin Xkid is essential for metaphase chromosome alignment and must be degraded to allow anaphase chromosome movement. Cell *102*, 411–424.

Hetzer, M.W., Walther, T.C., and Mattaj, I.W. (2005). Pushing the envelope: structure, function, and dynamics of the nuclear periphery. Annu. Rev. Cell Dev. Biol. *21*, 347–380.

Hinkle, B., Slepchenko, B., Rolls, M.M., Walther, T.C., Stein, P.A., Mehlmann, L.M., Ellenberg, J., and Terasaki, M. (2002). Chromosomal association of Ran during meiotic and mitotic divisions. J. Cell Sci. *115*, 4685–4693.

Lemaitre, J.M., Geraud, G., and Mechali, M. (1998). Dynamics of the genome during early Xenopus laevis development: karyomeres as independent units of replication. J. Cell Biol. *142*, 1159–1166.

Levesque, A.A., and Compton, D.A. (2001). The chromokinesin Kid is necessary for chromosome arm orientation and oscillation, but not congression, on mitotic spindles. J. Cell Biol. *154*, 1135–1146.

Montag, M., Spring, H., and Trendelenburg, M.F. (1988). Structural analysis of the mitotic cycle in pre-gastrula Xenopus embryos. Chromosoma *96*, 187–196.

Mora-Bermudez, F., Gerlich, D., and Ellenberg, J. (2007). Maximal chromosome compaction occurs by axial shortening in anaphase and depends on Aurora kinase. Nat. Cell Biol. *9*, 822–831.

Munne, S., and Cohen, J. (1998). Chromosome abnormalities in human embryos. Hum. Reprod. Update *4*, 842–855.

Nagy, A., Gertsenstein, M., Vintersten, K., and Behringer, R. (2003). Manipulating the Mouse Embryo. A Laboratory Manual (Cold Spring Harbor, NY: Cold Spring Harbor Laboratory Press).

Newport, J., and Dasso, M. (1989). On the coupling between DNA replication and mitosis. J. Cell Sci. Suppl. *12*, 149–160.

Newport, J., and Kirschner, M. (1982). A major developmental transition in early Xenopus embryos: II. Control of the onset of transcription. Cell *30*, 687–696.

O'Farrell, P.H., Stumpff, J., and Su, T.T. (2004). Embryonic cleavage cycles: how is a mouse like a fly? Curr. Biol. *14*, R35–R45.

Ohsugi, M., Tokai-Nishizumi, N., Shiroguchi, K., Toyoshima, Y.Y., Inoue, J., and Yamamoto, T. (2003). Cdc2-mediated phosphorylation of Kid controls its distribution to spindle and chromosomes. EMBO J. *22*, 2091–2103.

Onishi, M., Kinoshita, S., Morikawa, Y., Shibuya, A., Phillips, J., Lanier, L.L., Gorman, D.M., Nolan, G.P., Miyajima, A., and Kitamura, T. (1996). Applications of retrovirus-mediated expression cloning. Exp. Hematol. *24*, 324–329.

Sakai, K., and Miyazaki, J. (1997). A transgenic mouse line that retains Cre recombinase activity in mature oocytes irrespective of the cre transgene transmission. Biochem. Biophys. Res. Commun. *237*, 318–324.

Shiroguchi, K., Ohsugi, M., Edamatsu, M., Yamamoto, T., and Toyoshima, Y.Y. (2003). The second microtubule-binding site of monomeric kid enhances the microtubule affinity. J. Biol. Chem. *278*, 22460–22465.

Siracusa, G., Whittingham, D.G., and De Felici, M. (1980). The effect of microtubule- and microfilament-disrupting drugs on preimplantation mouse embryos. J. Embryol. Exp. Morphol. *60*, 71–82.

Todaro, G.J., and Green, H. (1963). Quantitative studies of the growth of mouse embryo cells in culture and their development into established lines. J. Cell Biol. *17*, 299–313.

Tokai, N., Fujimoto-Nishiyama, A., Toyoshima, Y., Yonemura, S., Tsukita, S., Inoue, J., and Yamamota, T. (1996). Kid, a novel kinesin-like DNA binding protein, is localized to chromosomes and the mitotic spindle. EMBO J. *15*, 457–467.

Tokai-Nishizumi, N., Ohsugi, M., Suzuki, E., and Yamamoto, T. (2005). The chromokinesin Kid is required for maintenance of proper metaphase spindle size. Mol. Biol. Cell *16*, 5455–5463.

Vagnarelli, P., Hudson, D.F., Ribeiro, S.A., Trinkle-Mulcahy, L., Spence, J.M., Lai, F., Farr, C.J., Lamond, A.I., and Earnshaw, W.C. (2006). Condensin and Repo-Man-PP1 co-operate in the regulation of chromosome architecture during mitosis. Nat. Cell Biol. *8*, 1133–1142.

Yamagata, K., Yamazaki, T., Yamashita, M., Hara, Y., Ogonuki, N., and Ogura, A. (2005). Noninvasive visualization of molecular events in the mammalian zygote. Genesis *43*, 71–79.

Yoshida, Y., Nakamura, T., Komoda, M., Satoh, H., Suzuki, T., Tsuzuku, J.K., Miyasaka, T., Yoshida, E.H., Umemori, H., Kunisaki, R.K., et al. (2003). Mice lacking a transcriptional corepressor Tob are predisposed to cancer. Genes Dev. *17*, 1201–1206.

Zhang, C., and Clarke, P.R. (2000). Chromatin-independent nuclear envelope assembly induced by Ran GTPase in Xenopus egg extracts. Science *288*, 1429–1432.

Zhang, C., and Clarke, P.R. (2001). Roles of Ran-GTP and Ran-GDP in precursor vesicle recruitment and fusion during nuclear envelope assembly in a human cell-free system. Curr. Biol. *11*, 208–212.

Zhu, C., Zhao, J., Bibikova, M., Leverson, J.D., Bossy-Wetzel, E., Fan, J.B., Abraham, R.T., and Jiang, W. (2005). Functional analysis of human microtubule-based motor proteins, the kinesins and dyneins, in mitosis/cytokinesis using RNA interference. Mol. Biol. Cell *16*, 3187–3199.